Photosynthesis

DOI: 10.1002/anie.201210228

Silicon Nanowires Show Improved Performance as Photocathode for Catalyzed Carbon Dioxide Photofixation**

Rui Liu, Carolynn Stephani, Jae Jin Han, Kian L. Tan, and Dunwei Wang**

The ability to use sunlight, the most abundant form of energy on earth's surface, to power chemical reactions is a unique feature of natural photosynthesis.[1] The process enables the storage of solar energy that is intermittent in nature. With carbon dioxide (CO_2) as a feedstock, it also produces highly specific organic chemicals that are the essential energy suppliers or building blocks for a wide range of important natural processes.[2–4] Significant research efforts have been devoted to mimicking the process in artificial systems, the major focus being on how to improve solar energy conversion efficiencies.[5,6] Relatively underwhelming attention is paid to issues related to low product specificities when CO_2 is reduced. Inspired by the detailed mechanisms of the dark reactions in the Calvin cycle,[7] we recently reported a strategy to combat this problem.[8] Briefly, the key was to avoid direct reduction of CO_2, which is prone to produce carbon atoms of varying oxidation states. Instead, we rely on the creation of an intermediate that subsequently reacts with CO_2 selectively. The idea is similar to the approach of Bocarsly et al. using pyridinium for the production of methanol,[6] although we seek to produce more complex and hence synthetically relevant organic molecules. In principle, the scope of reactions can be significantly broadened if the intermediate produced by photoreduction is a catalyst that can be used to react with CO_2 to yield the desired product. Similar to photosynthesis, the carbon–carbon bond-forming reactions are independent of photons (e.g. the dark reactions), allowing for an improved control in selectivity. To test this hypothesis, here we report our success in performing CO_2 photofixation with the help of the $[Ni(bpy)_2]$ catalyst. To our surprise and delight, we observed that the Si nanowire (SiNW) photoelectrode exhibited more than 300 mV turn-on potential increase when compared with planar Si. We attributed this to the multifaceted nature of the nanowires.

Our catalyzed CO_2 photofixation design is shown in Scheme 1. SiNWs absorb solar energy and excite electrons to the conduction band. The excited electrons are transferred to the $[Ni^{II}(bpy)_2]^{2+}$ complex and produce $[Ni^{0}(bpy)_2]$, which then binds with CO_2 and the alkyne substrate. Oxidative

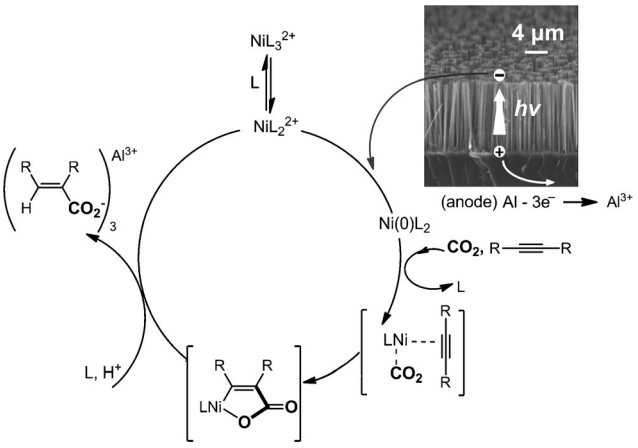

Scheme 1. Proposed reaction mechanism of catalyzed CO_2 fixation by Si photoelectrodes.

cyclization of the alkyne and CO_2 yields a Ni^{II} metallacycle, which upon protonation releases the desired carboxylic acid, regenerating the Ni^{II} catalyst. Overall, the Ni-catalyzed process provides an efficient and stereospecific synthesis of trisubstituted alkenes from CO_2 and an alkyne.

Although the process may be accomplished by electrochemistry[9] using, for example, Pt as the working electrode, the advantage of performing the reaction on a Si photoelectrode is a significantly lowered requirement for externally applied potentials, as shown in Figure 1. Analysis of the crude reaction mixture shows that the reaction proceeded at 81% faradaic efficiency for the carboxylated product. Most prom-

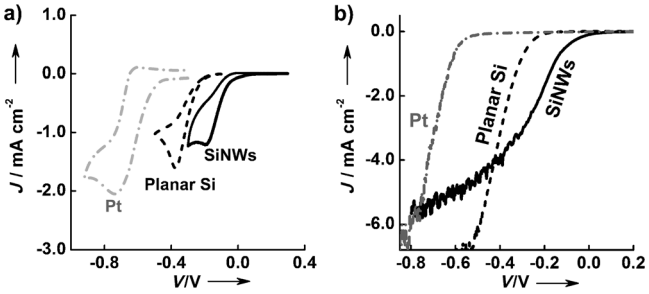

Figure 1. Comparison of various electrodes and photoelectrodes. a) Cyclic voltammetry in acetonitrile with 0.1 M tetrabutylammonium bromide, 5 mM $[Ni(bpy)_3(BF_4)_2]$, and 0.05 M 4-octyne, saturated with CO_2. Scan rate: 50 $mV s^{-1}$. Both SiNW and planar Si photoelectrodes were under illumination of a Xenon lamp (light intensity adjusted to 100 $mW cm^{-2}$). No measurable current was observed on the SiNWs and planar Si photoelectrodes without illumination. b) Polarization curves in the same solution but under vigorous stiring (1000 rpm).

[*] R. Liu, C. Stephani, J. J. Han, Prof. Dr. K. L. Tan, Prof. Dr. D. Wang
Department of Chemistry, Boston College
Merkert Chemistry Center, Chestnut Hill, MA 02467 (USA)
E-mail: kian.tan@bc.edu
dunwei.wang@bc.edu

[**] The project is supported in part by the NSF (grant number DMR 1055762) to D.W. and the NIGMS (grant number R01GM08758) to K.L.T. D.W. and K.L.T. are both Alfred P. Sloan Fellows.

Supporting information for this article is available on the WWW under http://dx.doi.org/10.1002/anie.201210228.

inent of the features are that the peaks in the cyclic voltammetry (CV) corresponding to the reduction/oxidation of $[Ni^{II}(bpy)_2]^{2+}/[Ni^0(bpy)_2]$ are anodically shifted, from −0.71 V for Pt to −0.37 V for a planar Si photoelectrode, and −0.19 V for SiNWs (Figure 1a; all potentials shown herein are relative to the Ag/AgI/I^- reference electrode, which is −0.56 V relative to the saturated calomel electrode (SCE); see the Supporting Information). The shift suggests that the need for applied potentials is greatly reduced, with the additional power produced by the photoelectrode. Our approach allows one to effectively use the energy delivered by light for the reduction of CO_2, which is an important character of photosynthesis. We also note that there are no anodic peaks visible on all electrodes (Figure 1a), indicating electron transfer from Ni^0 to an alkyne and CO_2 as proposed in Scheme 1. Without alkyne and CO_2, the anodic peaks were unambiguously observed (see the Supporting Information).

There are several points we wish to highlight in this paper, including the importance of light, the performance difference between electrodes made of SiNWs and planar Si, and a hypothesis for these unusual observations. We first focus on the effect of light on the reactions. Within the potential window that we measured (Figure 1), without light no currents were observed on electrodes made of Si, either planar or SiNWs. The result suggests that light plays an important role in powering the reactions. The difference between the red/ox potentials of $[Ni^{II}(bpy)_2]^{2+}/[Ni^0(bpy)_2]$ for Si and that for Pt was inferred as the photovoltage provided by Si.[10] When Si is in equilibrium with the electrolyte system, a downward band bending occurs (see Figure 2c&d). This is because the Fermi level (as measured by the flatband potential, V_{fb}) of Si is more positive than the equilibrium potential of the $[Ni^{II}(bpy)_2]^{2+}/[Ni^0(bpy)_2]$ system. Here we emphasize that the exact equilibrium potentials of the electrolyte system relative to the Fermi levels of Si are unknown. The measurement of these values requires further research. It is likely to be different from the red/ox peak positions of $[Ni^{II}(bpy)_2]^{2+}/[Ni^0(bpy)_2]$ as measured by the CV peak positions in Figure 1a, which were obtained under stagnant conditions. This is because the equilibrium potential of $[Ni^{II}(bpy)_2]^{2+}/[Ni^0(bpy)_2]$ depends on the relative concentrations of the oxidized and reduced species. As such, our representation of the band-bending in Figure 2 is qualitative in nature.

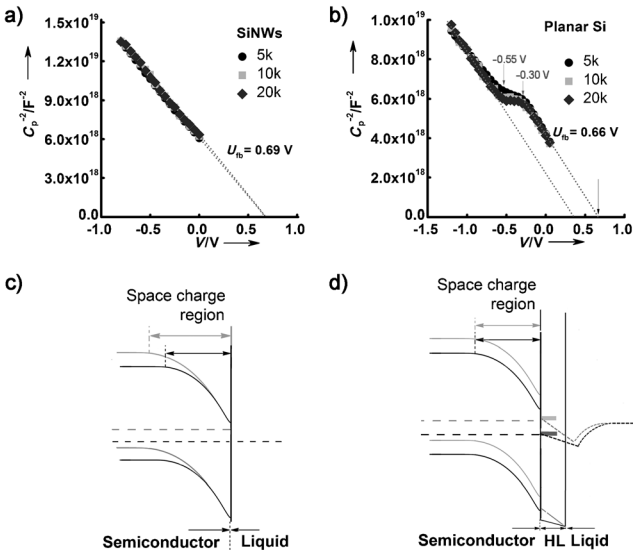

Figure 2. Mott–Schottky plots and the corresponding energy band diagrams of SiNWs electrodes (a and c, respectively) and planar Si (b and d, respectively). The insets in (a) and (b) show the legends of the frequencies used. The plateau observed on planar Si (b) is attributed to the charging of the Helmholtz (HL) layer. The understanding is shown in panel (d).

The data presented in Figure 1a nonetheless allowed us to obtain a V_{ph} of 0.34 V for planar Si and one of 0.52 V for SiNWs. These values fall in the range of photovoltages observed on both n- and p-type Si previously.[11,12] What was intriguing, however, is the difference between photoelectrodes made of planar Si and SiNWs. To better present the difference, typical polarization curves for all three types of electrodes are plotted in Figure 1b. If we define the potential at which the currents (or photocurrents) reach 50 μA cm^{-2} as the turn-on voltage (V_{on}), the value for Pt is −0.46 V, and those for planar Si and SiNWs are −0.20 V and +0.04 V, respectively. The result implies photoelectrodes of SiNWs produce larger photovoltages. While reduced reflection and improved light harvesting by SiNWs might contribute to the greater photovoltage,[13] such an effect would fail to account for a significant difference like the one that we observe (0.24 V more photovoltage measured on SiNWs). The same trend was observed on more than six pairs of photoelectrodes, with less than 0.02 V differences in the photovoltages measured. We therefore ruled out the possibilities of measurement artifacts.

We suggest that the difference is a manifestation of how easy or difficult charge is transferred between Si and the catalyst. It is well documented that the impedance to the charge-transfer process are observed in polarization curves as a part of the overpotential.[14] Because $[Ni(bpy)_2]^{2+/0}$ is not known to form covalent bonds with Si, the electron transfer likely proceeds through an outer-sphere mechanism. The ease (or difficulty) of electron transfer to $[Ni(bpy)_2]^{2+/0}$ is dependent on which surfaces of Si it is exposed to and how the molecules are arranged relative to Si surface atoms. The advantage of SiNWs is that each individual nanowire is multifaceted, meaning that a variety of crystal planes are present. It is reasonable to assume that electron transfer pathways between a SiNW and a $[Ni(bpy)_2]^{2+}$ are preferably formed on a crystal plane that favors the process, more so than on one that requires higher overpotentials, such as the (100) faces.

One way to test this hypothesis is to examine the electrochemical impedance spectroscopy. For this purpose, we plot how the capacitance varies with the applied potentials in the dark. As shown in Figure 2a, a Mott–Schottky (M-S) relationship [Eq. (1)]

$$C_{SC}^{-2} = \frac{2}{A_S^2 q \varepsilon_0 \varepsilon N_A}\left(V_{fb} - V - \frac{kT}{q}\right) \quad (1)$$

is followed by the SiNWs for frequencies ranging between 5000, 10000, and 20000 Hz. Here, C represents the space

charge capacitance in the semiconductor, N_A is the hole density, q is the electron charge, ε_0 is vacuum permittivity of a vacuum, ε is the dielectric constant of Si, V is the applied potential, V_{fb} is the flat band potential, T is the temperature, and k is the Boltzmann constant. The negative slope proves that the majority carrier is a hole, consistent with the fact that p-type Si was used. From the M-S plots, a carrier concentration of $N_A = 3.1 \times 10^{15}\ cm^{-3}$ and $V_{fb} = +0.69$ V was obtained. The carrier concentration calculation is in excellent agreement with the information provided by the vendor of the Si substrate (resistivity: 10–20 Ω cm; $N_A = 10^{15}\ cm^{-3}$).

In stark contrast, a plateau shows up in the M-S plots for planar Si between −0.55 to −0.30 V. In the literature, a plateau like this is typically understood as a voltage region within which the applied potential drops within the Helmholtz layer instead of in the depletion region of the semiconductor.[15] The most common cause for such a phenomenon has been regarded as surface states-induced Fermi level pinning.[16] We, however, consider surface states trapping an unlikely mechanism for the phenomenon because the plateau was only observed on pristine planar Si; it was absent on SiNWs produced by chemical etching which are far more likely to be of high surface states. We understand the origin of the plateau as the change of the Helmholtz layer on planar Si between −0.55 and −0.30 V. It is hypothesized that the arrangement of $[Ni^{II}(bpy)_2]^{2+}$ on Si surfaces is dependent on the surface potentials, and that the arrangement defines the impedance of charge transfer. For SiNWs, owing to the availability of a variety of facets, one that favors charge transfer between $[Ni^{II}(bpy)_2]^{2+}$ and Si is present within the entire potential window. For planar Si, on the other hand, the only available crystal plane is Si(100), which does not favor charge transfer between $[Ni^{II}(bpy)_2]^{2+}$ and Si above −0.30 V. Starting from −0.30 V, the negative potential induces molecular rearrangement for improved charge transfer, and the process is complete at −0.55 V. In other words, between −0.30 and −0.55 V, most of the applied potential drops within the Helmholtz layer instead of the space charge region of Si. The understanding is depicted in Figure 2 d. Close examination of the M-S plots of planar Si revealed that if the data between $V_{applied} = 0$ and −0.30 V are used to extract the V_{fb}, a value of +0.66 V is obtained, which is only different from that obtained on SiNWs by 0.03 V (V_{fb} of a SiNW is +0.69 V, as shown in Figure 2 a). At applied potentials below −0.55 V, the potential drops by approximately 0.25 V within the Helmholtz layer that does not contribute to the formation of the space charge region. Note that all results discussed in this paragraph were obtained under steady-state conditions in the dark.

To validate the hypothesis, we further examined the Nyquist plots at different applied potentials by fitting the data using equivalent circuits (Figure 3; also see the Supporting Information). Two distinct features of this group of data are noted. First, the capacitance attributed to the space charge region of the SiNWs decreased monotonically between 0 and −0.600 V. By comparison, the capacitance corresponding to the space charge region of planar Si remained unchanged between −0.30 and −0.50 V. This observation is consistent with the M-S plots as shown in Figure 2. It proves that within this potential window, the increased negative potential on planar Si drops within the solution but not in the space charge region, as indicated in Figure 2 d. Second, a clear difference between the data obtained on SiNWs and those on planar Si is observed in the low frequency region, where the characteristics of the Helmholtz layer and the solution dominate the features. For instance, at 0 V the fitting of the data for planar Si resulted in a resistor of $4.03 \times 10^6\ \Omega$ while that for the SiNWs was $8.83 \times 10^4\ \Omega$. At −0.60 V, the values were 1.49×10^5 and $1.60 \times 10^5\ \Omega$, respectively (see the Supporting Information). The difference indicates that charge transfer from planar Si to $[Ni^{II}(bpy)_2]^{2+}$ at small applied potentials (e.g., 0 V) was indeed more difficult than that from SiNWs to $[Ni^{II}(bpy)_2]^{2+}$, whereas the difference is negligible at high applied potentials (e.g., −0.60 V).

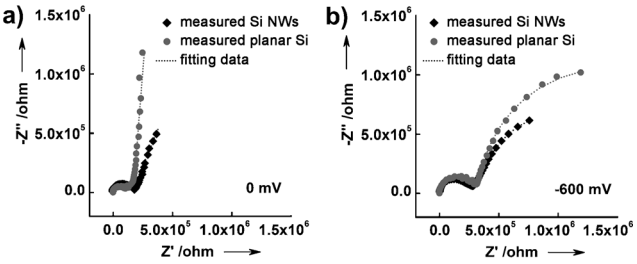

Figure 3. Nyquist plots at 0 V (a) and −0.600 V (b) for SiNWs (black) and planar Si (gray). The dotted lines are fitted to the data.

Taken as a whole, we understand the data as follows. When $[Ni^{II}(bpy)_2]^{2+}$ is in contact with SiNWs, a charge-transfer pathway is established at relatively positive potentials because of the multifaceted nature of the SiNWs. At similar potentials, a significant resistance between planar Si and $[Ni^{II}(bpy)_2]^{2+}$ exists, which disappears when the applied potential is negative enough (lower than −0.50 V, for example). The understanding also explains the photocurrent differences as shown in Figure 1 b. At −0.20 V applied potential, a current density of $-1.72\ mA\,cm^{-2}$ was observed on SiNWs while no photocurrent was measured on planar Si. In the diffusion-limited region (e.g., −0.60 V), higher photocurrents were measured on planar Si than on SiNWs because of better ionic diffusion on a planar electrode.

As Si is an earth abundant element, and a great deal of knowledge about its optoelectronic and photoelectrochemical properties has been accumulated, research on using Si-based materials for solar energy applications is of special interest. Within this context, our result is significant. It shows that SiNWs may exhibit advantages over planar Si in addition to better light absorption. By reducing the overpotential because of charge transfer impedance, a higher photovoltage is measured on SiNWs than on planar Si. Although similar observations have been made by earlier reports,[17,18] little attention has been paid to explaining the phenomenon. To the best of our knowledge, our report is the first to systematically compare photoelectrodes of SiNWs and planar Si in a synthetically useful system. A consistent trend, albeit in a much less pronounced magnitude, was observed in our proof-of-concept demonstration of the benzophonene system.[8] Previous considerations[13,19,20] about the trade-off between

photovoltage reduction caused by surface states and better charge collection by the NW morphology are generally valid. Nevertheless, cautions must be used when applying these considerations to specific chemical systems as these factors may be outplayed by those related to the detailed chemical mechanisms. With the intense research attention on solar energy applications by photoelectrochemical processes, we envision that reactions similar to natural photosynthesis, that is, those seeking to use solar energy to produce highly specific chemicals, will gain increasingly more attention. For these reactions, each system must be evaluated individually.

Communicating the point that the multifaceted nature of SiNWs may be advantageous for catalytic photoelectrochemical processes is our primary intention. To fully understand the nature of the interface between Si and the electron-receiving groups, more detailed research is needed. For instance, Si with different crystal faces exposed could be obtained or produced and the charge-transfer characteristics could be measured to identify which facets favor charge transfer between Si and $[Ni^{II}(bpy)_2]^{2+}$. Detailed knowledge like this will contribute significantly to the goal of designing highly specific reactions that are powered by sunlight and produce useful chemicals in a way similar to natural photosynthesis but at much higher efficiencies.

Experimental Section

Photoelectrochemical (PEC) and electrochemical impedance spectroscopy (EIS) experiments were carried out using a CHI 609D Potentiostat. A three-electrode configuration was used, in which a Ag/AgI wire soaked in 0.1M tetrabutylammonium iodide acetonitrile solution was used as the reference electrode, a piece of high-purity Al foil (99.9995%, Alfa Aesar, USA) served as the counter electrode, and SiNW-based (fabrication details in the Supporting Information) or planar Si photoelectrodes were used as the working electrode. The electrolyte solution was composed of 5 mM $[Ni(bpy)_3(BF_4)_2]$ catalyst and 0.1M tetrabutyl ammonium bromide (TBAB) ($\geq$ 99.0%, Sigma–Aldrich, USA) in 20 mL acetonitrile. CO_2 (Airgas, USA; flow rate: 120 SCCM) was continuously bubbled through the solution. A 150 W Xenon lamp (model 71228, Newport, USA) equipped with an AM 1.5G filter and illumination intensity calibrated to be 100 mW cm^{-2} by a Si photodiode (UV 005, OSI, Optoelectronic, USA) was used as the light source. The scan rates for both CV and IV curves were 50 mV s^{-1}. EIS measurement was done with electrolyte solution of 5 mM $Ni(bpy)_3(BF_4)_2$ catalyst and 0.1M tetrabutyl ammonium bromide in 20 mL acetonitrile without illumination. Frequency range was from 10^5 Hz to 1 Hz.

Received: December 21, 2012
Published online: March 7, 2013

Keywords: carbon dioxide fixation · catalysts · nanowires · photosynthesis · silicon

[1] R. E. Blankenship, D. M. Tiede, J. Barber, G. W. Brudvig, G. Fleming, M. Ghirardi, M. R. Gunner, W. Junge, D. M. Kramer, A. Melis, T. A. Moore, C. C. Moser, D. G. Nocera, A. J. Nozik, D. R. Ort, W. W. Parson, R. C. Prince, R. T. Sayre, *Science* **2011**, *332*, 805 – 809.
[2] A. J. Morris, G. J. Meyer, E. Fujita, *Acc. Chem. Res.* **2009**, *42*, 1983 – 1994.
[3] E. E. Benson, C. P. Kubiak, A. J. Sathrum, J. M. Smieja, *Chem. Soc. Rev.* **2009**, *38*, 89 – 99.
[4] N. Hoffmann, *Chem. Rev.* **2008**, *108*, 1052 – 1103.
[5] A. Bar-Even, E. Noor, N. E. Lewis, R. Milo, *Proc. Natl. Acad. Sci. USA* **2010**, *107*, 8889 – 8894.
[6] E. Barton Cole, P. S. Lakkaraju, D. M. Rampulla, A. J. Morris, E. Abelev, A. B. Bocarsly, *J. Am. Chem. Soc.* **2010**, *132*, 11539 – 11551.
[7] K. J. Dietz, U. Heber, *Biochim. Biophys. Acta Bioenerg.* **1986**, *848*, 392 – 401.
[8] R. Liu, G. Yuan, C. Joe, T. Lightburn, K. Tan, D. Wang, *Angew. Chem.* **2012**, *124*, 6813 – 6816; *Angew. Chem. Int. Ed.* **2012**, *51*, 6709 – 6712.
[9] S. Derien, E. Dunach, J. Perichon, *J. Am. Chem. Soc.* **1991**, *113*, 8447 – 8454.
[10] A. P. Goodey, S. M. Eichfeld, K. Lew, J. M. Redwing, T. E. Mallouk, *J. Am. Chem. Soc.* **2007**, *129*, 12344 – 12345.
[11] E. Warren, S. Boettcher, M. Walter, H. Atwater, N. Lewis, *J. Phys. Chem. C* **2011**, *115*, 594 – 598.
[12] M. Rosenbluth, C. Lieber, N. Lewis, *Appl. Phys. Lett.* **1984**, *45*, 423 – 425.
[13] E. Garnett, P. Yang, *Nano Lett.* **2010**, *10*, 1082 – 1087.
[14] A. J. Bard, L. R. Faulkner, *Electrochemical methods: fundamentals and applications*, Wiley, New York, **1980**.
[15] S. R. Morrison, *Electrochemistry at Semiconductor and Oxidized Metal Electrodes*, Plenum, New York, **1980**.
[16] N. S. Lewis, *Inorg. Chem.* **2005**, *44*, 6900 – 6911.
[17] Y. J. Hwang, A. Boukai, P. D. Yang, *Nano Lett.* **2009**, *9*, 410 – 415.
[18] I. Oh, J. Kye, S. Hwang, *Nano Lett.* **2012**, *12*, 298 – 302.
[19] B. M. Kayes, H. A. Atwater, N. S. Lewis, *J. Appl. Phys.* **2005**, *97*, 114302.
[20] S. W. Boettcher, E. L. Warren, M. C. Putnam, E. A. Santori, D. Turner-Evans, M. D. Kelzenberg, M. G. Walter, J. R. McKone, B. S. Brunschwig, H. A. Atwater, N. S. Lewis, *J. Am. Chem. Soc.* **2011**, *133*, 1216 – 1219.

